UNIVERSIDADE D COIMBRA FACULDADE DE MEDICINA

MESTRADO INTEGRADO EM MEDICINA – TRABALHO FINAL

ANA LÚCIA BATISTA OLIVEIRA

Communication between endothelial cells and cardiomyocytes: The role in Pulmonary Arterial Hypertension and in cardiomyocyte dysfunction.

ARTIGO CIENTÍFICO ORIGINAL

ÁREA CIENTÍFICA DE BIOLOGIA CELULAR

Trabalho realizado sob a orientação de:

CARLA ISABEL DOS SANTOS MARQUES

HENRIQUE MANUEL PAIXÃO DOS SANTOS GIRÃO

MARÇO/2020

Communication between endothelial cells and cardiomyocytes: The Role in Pulmonary Arterial Hypertension and in cardiomyocyte dysfunction.
Artigo científico original

Ana Lúcia Batista Oliveira[1]
Henrique Manuel Paixão dos Santos Girão[2]
Carla Isabel dos Santos Marques[2*]

[1] Faculdade de Medicina, Universidade de Coimbra, Portugal
[2] Instituto de Investigação Clínica e Biomédica de Coimbra (iCBR), Faculdade de Medicina, Universidade de Coimbra, Portugal

[*]cmarques@fmed.uc.pt
Polo III - Polo das Ciências da Saúde
Azinhaga de Santa Comba, Celas 3000-548
Coimbra

Trabalho final do 6.º ano médico com vista à atribuição do grau de mestre no âmbito do ciclo de estudos do Mestrado Integrado em Medicina.

Área científica: BIOLOGIA CELULAR
março 2020 | Coimbra

List of Abbreviations and Acronyms

BMPR2 Bone morphogenetic protein receptor type II
DAPI 4',6-diamidino-2-phenylindole
CM Conditioned medium
Cxs Connexins
ECs Endothelial cells
GJs Gap junctions
HUVECs Human umbilical vein endothelial cells
IKK Enzyme IκB kinase
LPS Lipopolysaccharide
LC3 Microtubule-associated protein 1A/1B-light chain 3
MCT Monocrotaline
mPAP Mean pulmonary arterial pressure
NF-κB Nuclear factor kappa-light-chain-enhancer of activated B cells
PAECs Pulmonary artery endothelial cells
PAH Pulmonary arterial hypertension
PASMCs Pulmonary artery smooth muscle cells
PAWP Pulmonary artery wedge pressure
PH Pulmonary hypertension
RV Right ventricular
RVH Right ventricular hypertrophy
UPS Ubiquitin-proteasome system

List of Illustrations

List of Tables

Resumo

Hipertensão arterial pulmonar (HAP) é uma doença crónica e progressiva caracterizada por um aumento persistente da resistência vascular pulmonar e pela sobrecarga do ventrículo direito, que resulta em insuficiência cardíaca e morte. O início e a progressão da HAP dependem da interação entre cardiomiócitos e células da vasculatura pulmonar, especialmente células endoteliais (ECs), que regulam a homeostasia vascular. No entanto, a interação entre esses tipos de células ainda é pouco conhecida, a nível molecular.

O presente estudo tem como objetivo avaliar a comunicação intercelular entre ECs e cardiomiócitos. Pelo facto de a inflamação estar associada à HAP, decidimos expor as células endoteliais da veia umbilical humana (HUVEC) ao lipopolissacarídeo (LPS), usado como um estímulo inflamatório. O meio condicionado recolhido das HUVEC foi adicionado a células H9c2, um modelo de cardiomiócitos. Posteriormente, foram avaliados os níveis de Cx43 e de marcadores de autofagia (i.e., p62 e a razão LC3II/LC3I) nas células. Os resultados mostraram que alterações do secretoma das HUVEC, induzidas pelo LPS modula os níveis de Cx43 e dos marcadores de autofagia em células H9c2. Resultados semelhantes foram observados *in vivo* utilizando um modelo animal de rato de PAH induzido por monocrotalina (MCT).

Estes resultados sugerem que, na HAP, as ECs secretam fatores para o sangue, nomeadamente mediadores inflamatórios, que afetam a função dos cardiomiócitos.

Palavras chaves

Autofagia; Comunicação Celular; Inflamação; Hipertensão Pulmonar.

Abstract

Pulmonary arterial hypertension (PAH) is a chronic and progressive disorder characterised by a persistent increase in pulmonary vascular resistance and overload of the right ventricle, leading to heart failure and death. The onset and progression of PAH depends on the crosstalk between cardiomyocytes and cells of the pulmonary vasculature, especially endothelial cells (ECs), which regulate vascular homeostasis. However, the interaction between these cell types is still poorly understood at a molecular level.

The present study aimed to evaluate the crosstalk between ECs and cardiomyocytes. We mimicked PAH-associated inflammation by exposing human umbilical vein endothelial cells (HUVEC) to the inflammatory stimulus lipopolysaccharide (LPS). The HUVEC-conditioned medium was then added to cardiac cell line (H9c2 cells). The levels of Cx43 and autophagy markers (i.e. p62 and LC3I/LC3II) in rat ventricular H9c2 cells exposed to a conditioned medium were evaluated. The results showed that conditioned medium from HUVECs modulated the levels of Cx43 and autophagy markers in H9c2 cells. Similar results were observed *in vivo* using a monocrotaline (MCT)-induced PAH rat model.

Together, these results suggest that in PAH, ECs secrete factors to the blood which are similar to inflammatory mediators, with these factors affecting cardiomyocyte function.

Keywords

Autophagy; Inflammation; Cell Communication; Pulmonary Hypertension.

Table of Contents

Chapter 1. Introduction

Pulmonary hypertension (PH) is a haemodynamic state defined as a mean pulmonary arterial pressure (mPAP) > 20 mmHg at rest, measured by right heart catheterisation (1). PH is a global health issue, with a prevalence of 10% in individuals aged over 65 years (2). Dyspnea, fatigue and syncope are the most common symptoms, with the interval between onset of these symptoms and diagnosis ranging from 18 to 32 months (2). Unfortunately, PH symptoms are associated with an impaired prognosis and the survival rate without treatment is 34% at 5 years (3). PH is categorised into five groups based on pathophysiological mechanisms, clinical features, haemodynamic characteristics and prognostic implications (1). PAH, described as a subgroup of PH by World Health Organization Group I PH (4), is characterised by mPAP > 20 mmHg, with normal pulmonary artery wedge pressure (PAWP) ≤ 15 mmHg and pulmonary vascular resistance (PVR) ≥ 3 Wood units, in the absence of other causes of pre-capillary PH (1, 5). PAH can be idiopathic, hereditary or secondary to various conditions, but all forms are a vasculopathy (4, 6), distinguished by endothelial dysfunction with an accumulation of vascular cells in the pulmonary arterial wall, loss of precapillary arteries, perivascular inflammation and fibrosis (7). Factors such as shear stress, hypoxia, dysregulation in bone morphogenetic protein receptor type II (BMPR2), metabolic derangements, mitochondrial dysfunction, circulating autoantibodies and immune complexes (7) lead to pulmonary vascular changes. Over time, these derangements impose a haemodynamic load on the right ventricle, leading to heart failure and death (8, 9). Right ventricular (RV) function is the primary and major prognostic factor for morbidity and mortality in PH. RV hypertrophy (RVH) is initially an adaptive physiological response to increased overload; however, with persistent afterload increase, this response transitions to pathological maladaptive remodelling (8). Furthermore, endothelial dysfunction eventually results in an imbalance between the production and release of several mediators, such as vasoconstrictors/vasodilators and proinflammatory/anti-inflammatory signals (10), which could modulate the integrity of RV function.

The electrical and metabolic coupling of cells through specialised cell contacts, called gap junctions (GJs), are critical for heart function (11). GJs localise mainly at the intercalated discs to allow rapid and unidirectional action potential propagation through the heart muscle (11-13). Therefore, the impairment of GJ intercellular communication has been associated with conduction block and arrhythmogenesis (13).

GJs are composed of a family of multispanning membrane proteins, the connexins (Cxs) (14). Cx43 is the most widely expressed and is found in a large variety of cell types and tissues (12), including ithe heart (11, 12, 15). Usually, in pathological conditions, Cx43 is down-regulated and/or redistributed to the lateral membranes of cardiomyocytes. In order to maintain the correct function of the heart, Cx43 needs to be carefully regulated (12). In the heart, autophagy and ubiquitin-proteasome system (UPS) are the two major intracellular pathways responsible for the degradation of most cellular proteins (15, 16), thus regulating the turnover of myocardial proteins(15). Its dysregulation has been associated with many pathological conditions, such as cancer (16), heart failure (10) and hypertension (14).

Despite many studies on PAH development (6), the effect of mediators released by pulmonary endothelium on cardiomyocytes remains underexplored. Therefore, this work focuses on the crosstalk between the endothelium and cardiomyocytes. To mimic pathological conditions, we exposed cardiomyocytes to the medium from ECs subject to inflammatory treatment. We aimed to evaluate the effect of this inflammatory treatment on autophagy and Cx43 expression in H9c2 cells, as well as in tissue extracts from a PH rat model. Improved knowledge of these processes may help in the designing of new and more effective approaches for PAH treatment.

Chapter 2. Materials and methods

2.1. Cell cultures

Human umbilical vein endothelial cells (HUVEC)/TERT2 cells were obtained from Everycyte. The cells were cultured in gelatin pre-coated flasks in Medium 200 (Thermo Fisher SCIENTIFIC) supplemented with Low Serum Growth Supplement (LSGS, Thermo Fisher SCIENTIFIC), 100 U/ml penicillin, 100 µg/ml streptomycin, 10% fetal bovine serum (FBS). Cells were grown under a humidified atmosphere, containing 5% CO_2 at 37°C.

The H9c2 rat cardiomyoblast cells were obtained from SIGMA-Aldrich and were obtained from ECACC and cultured in high glucose cultured in Dulbecco's modified Eagle's medium (DMEM), supplemented with 10% fetal bovine serum, 100 U/ml penicillin, 100 µg/ml streptomycin, 2 mM L-glutamine under a humidified atmosphere, containing 5% CO_2 at 37°C.

2.2. Conditioned medium (CM)

HUVECs were treated with LPS (Sigma-Aldrich) dissolved in saline solution for 24 hours. The medium was removed 6 hours before the end of experiment and replaced by new Medium 200, to remove any residual LPS. Then, the medium was collected (HUVECs conditioned medium, CM-HUVECs), centrifuged at 15,000 g for 5 minutes at 4°C to remove cell debris and stored at -80°C for subsequent experimentation.

2.3. H9c2 cells treatment

H9c2 cells were treated with CM-HUVECs for 24h under a humidified atmosphere containing 5% CO_2 at 37°C.

2.4. Cell viability assay

Cell viability was assessed by Alamar Blue (Resazurin) assay. Briefly, cells were treated with different concentrations (50 and 100 µg/ml) of LPS for 12, 24 and 48 hours. The cells were further incubated with resazurin (final concentration 50 µM) for 4 hours at 37 °C, after which the absorbance was recorded at 570 nm with a reference filter at 620 nm using Biotek Synergy HT spectrophotometer (Biotek). Cell viability (% control) was calculated according to the ratio between (A570 - A620) treated cells and (A570 - A620) control cells.

2.5. Pulmonary hypertension model

The animal model of PH was developed as described previously by Baptista *et al* (8). Briefly, PH was induced in rats by a single intraperitoneal injection (60 mg/Kg body weight) of MCT. Rats, euthanised by cervical dislocation, were sacrificed at 3, 4 and 6 weeks. All animal experiment protocols were approved by the ORBEA-IBILI (permit 09/2015) and handled according to European Union guidelines (2010/63/EU).

2.6. Western blot (WB) analysis

Total cell extracts were obtained by harvesting the cells in Laemmli buffer (4 % SDS, 20% glycerol, 10% 2-mercaptoethanol, 0.004% bromophenol blue, 0.125 M Tris-HCl, pH 6.8). Then cell lysates were sonicated and denaturated at 95°C for 5 minutes.

The right ventricle was homogenised in a tissue grinder (Potter-Elvehjem PTFE, Corning Life Sciences), in a lysis buffer (150 mM NaCl, 50 mM Tris-HCl, 1% NP-40 and 0.1%, 0,2 % SDS, pH 7.5) supplemented with protease and phosphatase inhibitors. Homogenates were centrifuged at 1000 g for 5 minutes, and further centrifuged at 15,700 g, for 20 minutes. The supernatants were denatured with 3x Laemmli buffer, boiled at 95ºC for 5 minutes, and sonicated.

Whole-cell and tissue extracts were resolved by SDS-PAGE and electrophoretically transferred onto nitrocellulose membranes. The membranes were blocked for 1 hour at room temperature with 5% non-fat milk in Tris-buffered saline-Tween 20 (TBS-T) (20 mM Tris-HCl, 150 mM NaCl and 0.2% Tween 20, pH 7.6) for 1 hour at room temperature, and then probed overnight at 4°C with the appropriate primary antibodies (Table I). Following incubation of primary antibodies, the blots were washed three times with TBS-T (15 minutes each) and incubated with horseradish peroxidase-conjugated for 1 hour at room temperature and then washed with TBS-T three times (15 minutes each). The immunoreactive proteins were detected by chemiluminescence (ImageQuantTM LAS 500, Amersham Biosciences). Immunoblot band intensity was analysed with Image J and calnexin was used as a protein loading control.

2.7. Immunofluorescence microscopy

H9c2 cells were grown on glass coverslips and treated with the CM. Cells were fixed with 4% paraformaldehyde (PFA) in phosphate-buffered Saline (PBS), for 10 minutes, washed three times with PBS, permeabilised with 0.2% (v/v) Triton X-100 in PBS for 5 minutes and blocked with 2% bovine serum albumin (BSA) in PBS for 30 minutes. Then, cells were probed with primary antibodies (Table 1) directed against Cx43 for 1 hour at room temperature, washed three times with PBS and probed with fluorescent-coupled secondary antibodies (Alexa Fluor 488).

Nuclei were stained with 4',6-diamidino-2-phenylindole (DAPI). The cells were rinsed in PBS and then mounted on microscope slides with MOWIOL 488 Reagent (Calbiochem). All solutions were prepared in 2% w/v BSA in PBS. Fluorescence images were obtained using a Zeiss Axio HXP IRE 2 microscope (Carl Zeiss AG).

Table 1 List of primary and secondary antibodies used for WB and immunofluorescence (IF).

Antibody	**Host/Clonality**	**Application**	**Dilution**	**Company**
Anti-IκBα	Rabbit/polyclonal	WB	1:1000	Cell Signalling Technology
Anti-Cx43	Goat/polyclonal	WB	1:5000	SICGEN
Anti-LC3	Rabbit/polyclonal	WB	1:1000	Thermo Fisher Scientific
Anti-p62	Rabbit/polyclonal	WB	1:1000	Cell Signalling Technology
Anti-Cx43	Goat/polyclonal	IF	1:100	SICGEN
Anti-calnexin	Goat/polyclonal	WB	1:5000	SICGEN
Anti-goat HRP	Rabbit/polyclonal	WB	1:10000	BioRad
Anti-rabbit HRP	Goat**/**polyclonal	WB	1:10000	BioRad
Alexa Fluor 488 anti-goat	Donkey/polyclonal	IF	1:200	Molecular Probes, Life Technologies

2.8. Statistical analysis.

Quantitative data are presented as the mean ± standard error. All experiments were repeated at least three times with similar results. Figures show data from one representative experiment. The number of repititions for each experiment is stated in each specific figure legend. Differences among multiple groups were analysed by one-way ANOVA or two-way ANOVA, followed by Dunnett's test for multiple comparisons. All computations were performed using GraphPad Prism 6.0 Software. In all experiments, differences were considered statistically significant at $p<0.05$.

Chapter 3. Results

3.1. Effect of LPS on cell viability and inflammation response on HUVECs

In this study, LPS was used to induce inflammation in ECs. To investigate the impact of LPS on HUVECs viability, resazurin reduction colourimetric assay was used. HUVECs were treated with LPS (50 and 100 µg/ml) for 12, 24 and 48 h. The cells were further incubated with resazurin (final concentration 50 µM) for 4 h. The results indicate that concentrations of LPS used have a non-cytotoxic effect on HUVECs (Figure 1.).

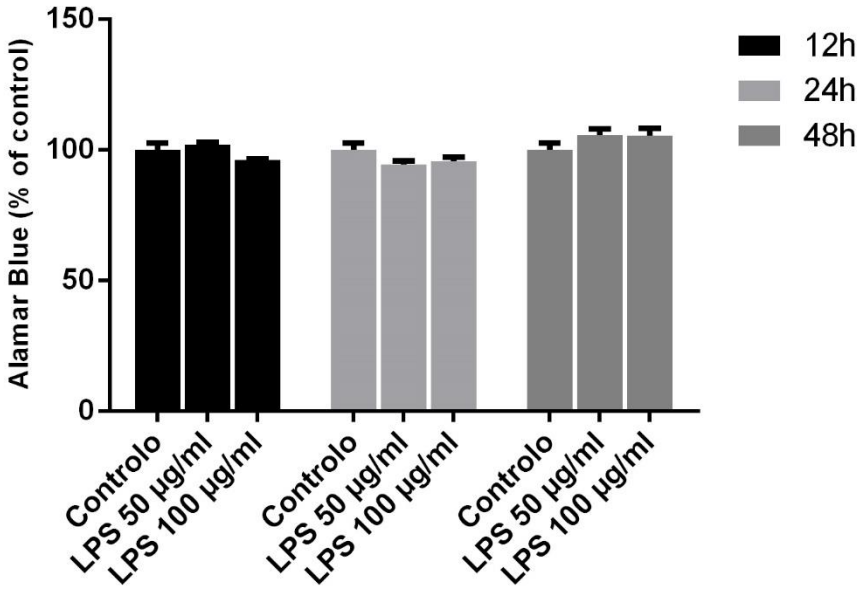

Figure 1. HUVECs cell viability. HUVECs were treated with LPS (50 and 100 µg/ml) for 12, 24 and 48 hours, and resazurin assay was used to assess cell viability. The percentage of cytotoxicity was calculated relative to a control (untreated cells). Data are expressed as the mean ± SEM (of at least three independent experiments performed in duplicate).

Several studies (17, 18) have demonstrated that nuclear factor kappa-light-chain-enhancer of activated B cells (NF-κB) transcription factor modulates the expression of genes implicated in inflammatory responses. The NF-κB activation involves the phosphorylation of IκBα, which results in IκBα ubiquitination and degradation by the proteasome (17, 18). Therefore, to assess LPS-mediated endothelial inflammation, we quantified the expression of IκBα. The results presented below in Figure 2 showed that, in cells treated with LPS, the protein levels of IκBα trended down, suggesting that IκBα in phosphorylated and degraded by the proteasome.

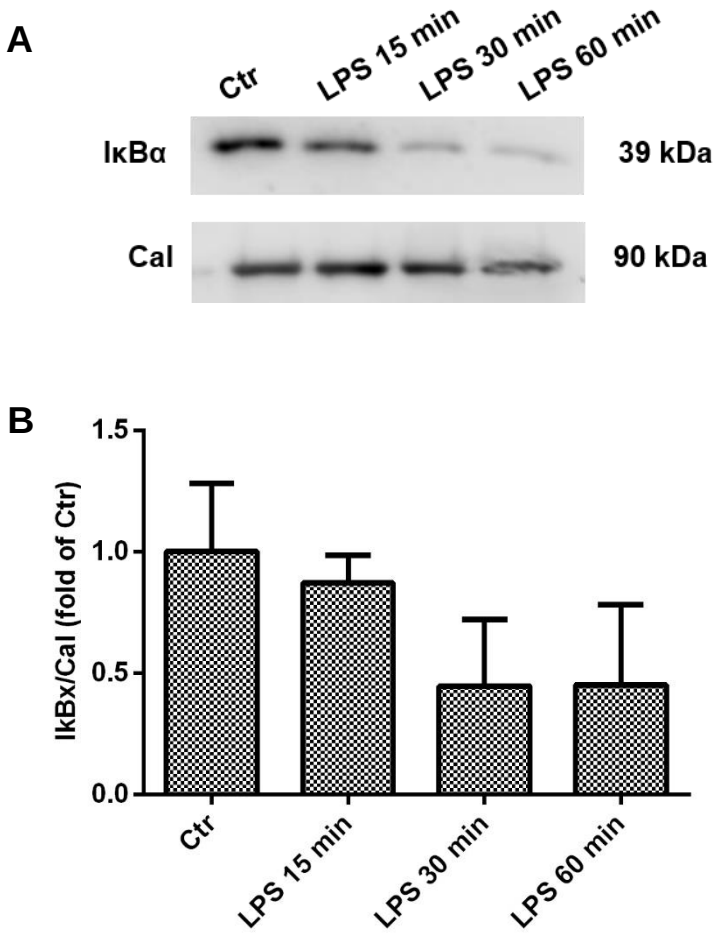

Figure 2. Expression of IκBα after LPS treatment. (A) HUVEC cells were treated with LPS treatment (100 µg/ml) for 15, 30 and 60 minutes. Whole-cell extracts were prepared and analysed by representative WB using anti–IkBα or anti-calnexin antibodies. (B) Densitometric quantification of IκBα expression using calnexin as a loading control (n=1).
Cal, Calnexin; Ctr, Control

3.2. Modulation of Cx43 and autophagy markers on H9c2 cells after treatment with CM-HUVECs

The major gap junction protein expressed in the heart, Cx43, is highly remodelled in the diseased heart (10). Usually, Cx43 undergoes a remodelling that involves its degradation and/or lateralisation at the lateral membranes. To evaluate the impact of the crosstalk between ECs and cardiomyocyte on Cx43 levels, CM was collected from HUVECs after an inflammatory stimulus using 50 or 100 µg/ml of LPS for 24 hours (CM-HUVECs-LPS). Therefore, we evaluated the effect of CM-HUVECs on H9c2 Cx43 levels. The results shown below demonstrate that the expression of Cx43 decreased significantly ($p<0.05$) in H9c2 cells (Figure 3).

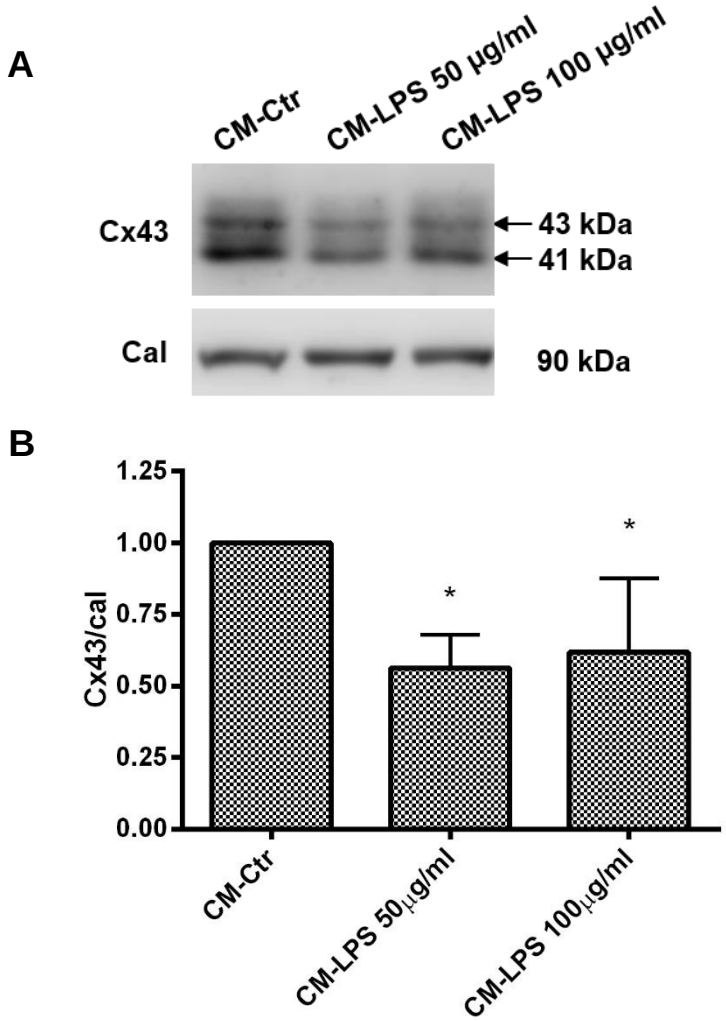

Figure 3. Effect of conditioned medium from HUVECs treated with LPS on Cx43 levels in H9C2 cells. (A) H9C2 cells treated with CM-HUVECs for 24 h. Whole-cell extracts were prepared and analyzed by representative WB using anti–Cx43 or anti-calnexin antibodies; (B) Densitometric quantification of Cx43 expression using calnexin as a loading control. Data are presented as the mean ± SEM of, at least, three independent experiments and are expressed as a percentage of the control. (*$p < 0.05$ vs. Ctr.)

Cal, Calnexin; Ctr, Control;

Immunofluorescence staining was then performed to evaluate the subcellular distribution of Cx43 in H9c2 cells after treatment with CM from HUVECs. The images obtained by fluorescent microscopy suggested that Cx43 appears to accumulate at the perinuclear region (Figure 4).

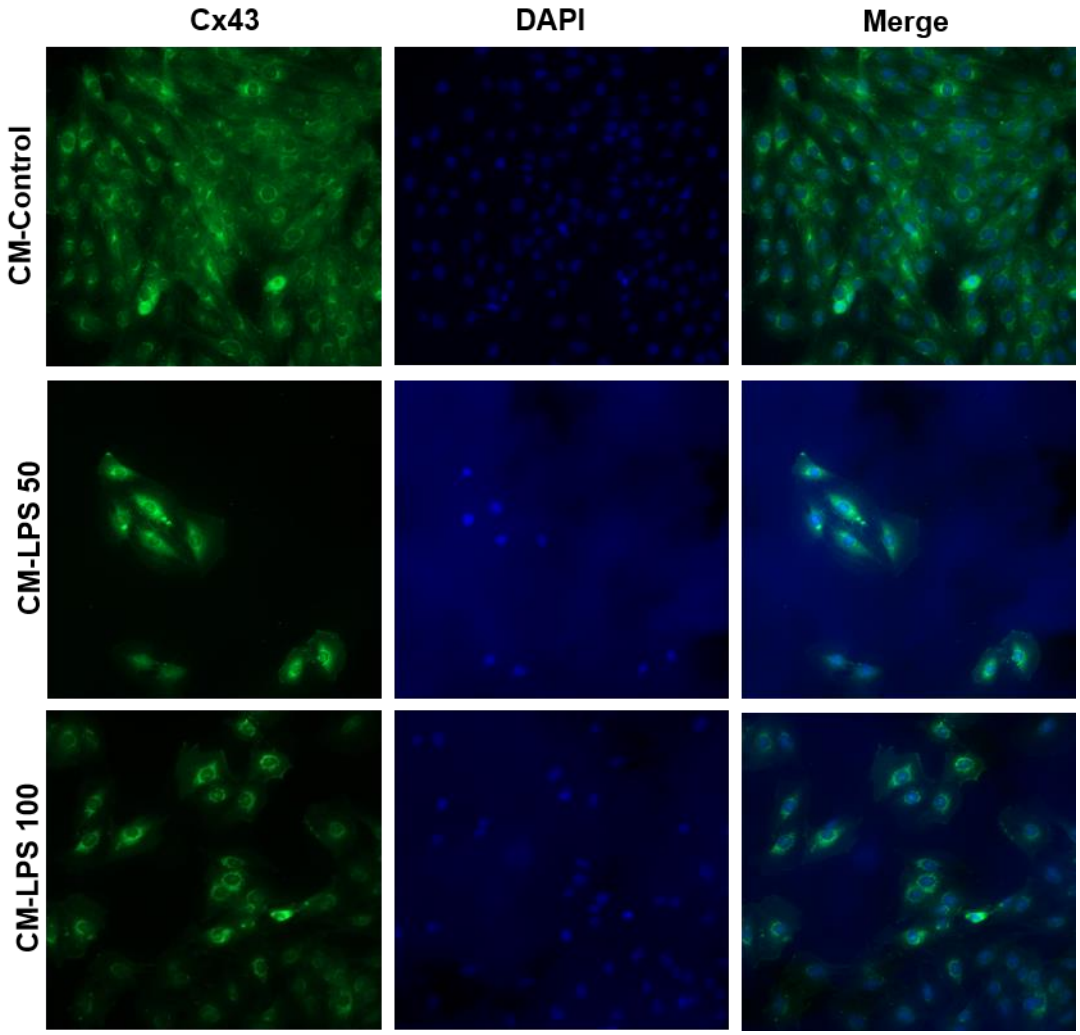

Figure 4. Modulation of Cx43 distribution by on H9c2 cells after treatment with CM-HUVECs treated with LPS. The subcellular distribution of Cx43 inH9c2 cells, treated with CM-HUVECs for 24 hours, was assessed using immunofluorescence assay. Representative immunofluorescence images with Cx43 (green) and nucleus (blue). All images were taken at 20x magnification (n=2).

Considering that autophagy and intercellular communication are dysregulated in PAH (2, 19, 20), we proceeded to investigate the effect of the medium from ECs on these biological processes. The expression levels of microtubule-associated protein 1A/1B-light chain 3 (LC3) and p62 levels in H9c2 cells after treatment with CM from ECs were evaluated using WB (Figure 5). Results showed an increased ratio of LC3-II/LC3-I (Figure 5A) and decrease in p62 levels (Figure 5C). These data suggest the activation of autophagy.

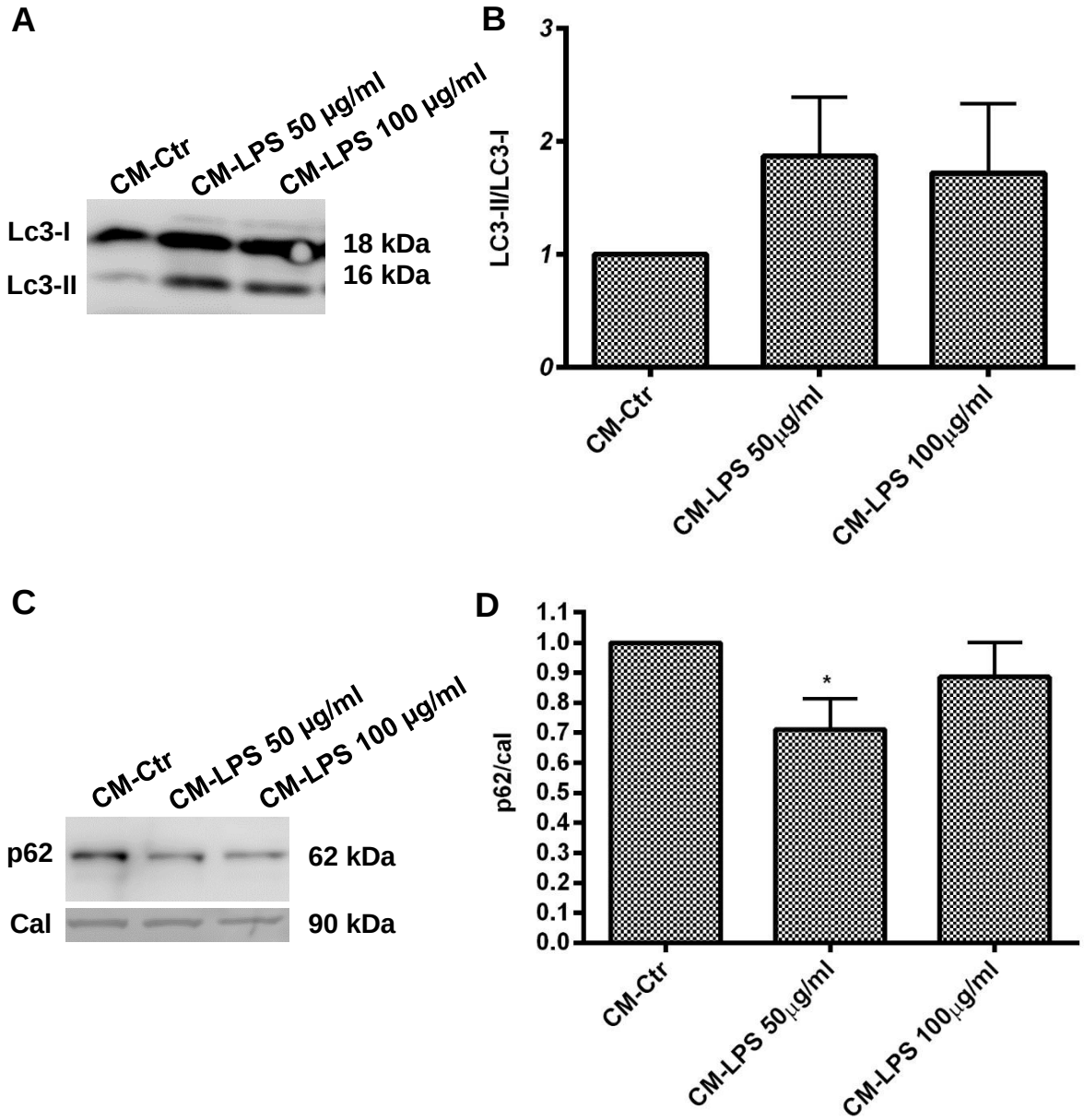

Figure 5. Effect of CM-HUVECs treated with LPS on H9C2 cells on autophagy activity in H9c2 cells. (A) CM-HUVECs were collected after LPS treatment (50 or 100 µg/ml) for 24 h. H9C2 cells treated with CM-HUVECs for 24 h. Whole-cell extracts were prepared and analyzed by representative WB using anti–LC3; (B) Densitometric quantification of ratio LC3II/LC3-I. Data are presented as the mean ± SEM of, at least 3 independent experiments and

are expressed as a percentage of the control. (C) Whole-cell extracts were prepared and analysed by representative WB using anti–p62 or anti-calnexin antibodies; (D) Densitometric quantification of p62 expression using calnexin as a loading control. Data are presented as the mean ± SEM of, at least, three independent experiments and are expressed as a percentage of control. (*p < 0.05. vs. Ctr.). Cal, Calnexin; Ctr, Control;

3.3. Modulation of Cx43, LC3 and p62 in the right ventricle of the MCT-treated rat

To investigate the modulation of proteins associated with intercellular communication and autophagy in the RVH, we used the established MCT rat model of PH(8). It has been reported that MCT rat model of PAH can partially reproduce the human phenotype of RVH progression, including the transition from an adaptive to a maladaptive phase (21), changes in gene expression and inflammatory activation (22). After MCT administration in animals, the RV initially compensates for the increase in afterload through hypertrophy and increased contractile function, known as the adaptative phase. After 3-4 weeks, with the disease progressing to a maladaptive phase, the RV's compensatory mechanisms fail, leading to RV failure and death (6, 8).

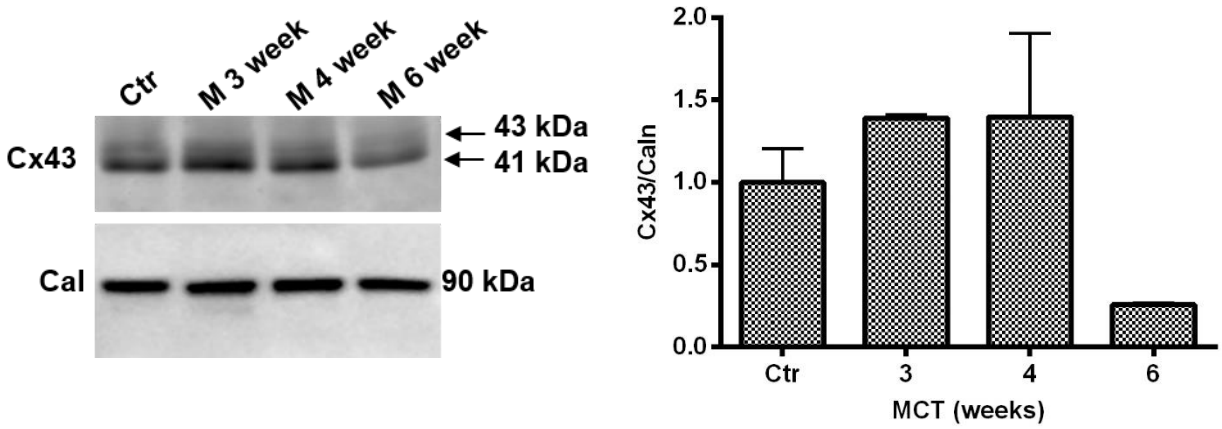

Figure 6. Effect on Cx-43 levels with progression of RV hypertrophy. RV homogenized from MCT-treated rat were prepared and analysed by WB using anti-Cx43 antibody and anti-calnexin antibody as a loading control. The Cx43 density was measured, plotted in a graph and normalised to calnexin. Representative immunoblots are presented above the graphs. Data are presented as the mean ± SEM of, at least 3 independent experiments and are expressed as a percentage of control.
Cal, Calnexin; Ctr, Control;

Our findings show that the expression level of Cx43 tends to increase three to four weeks after MCT injection and then decreases after this time (Figure 6). Regarding the ratio of LC3-II/LC3-I (Fig 7A), a marker of autophagy activity, the data suggested an increase with disease development. However, unlike as expected, the p62 levels (Fig 7B) the data suggest an increase in the maladaptive stage of the disease, but without any changes in the adaptative stage of the disease.

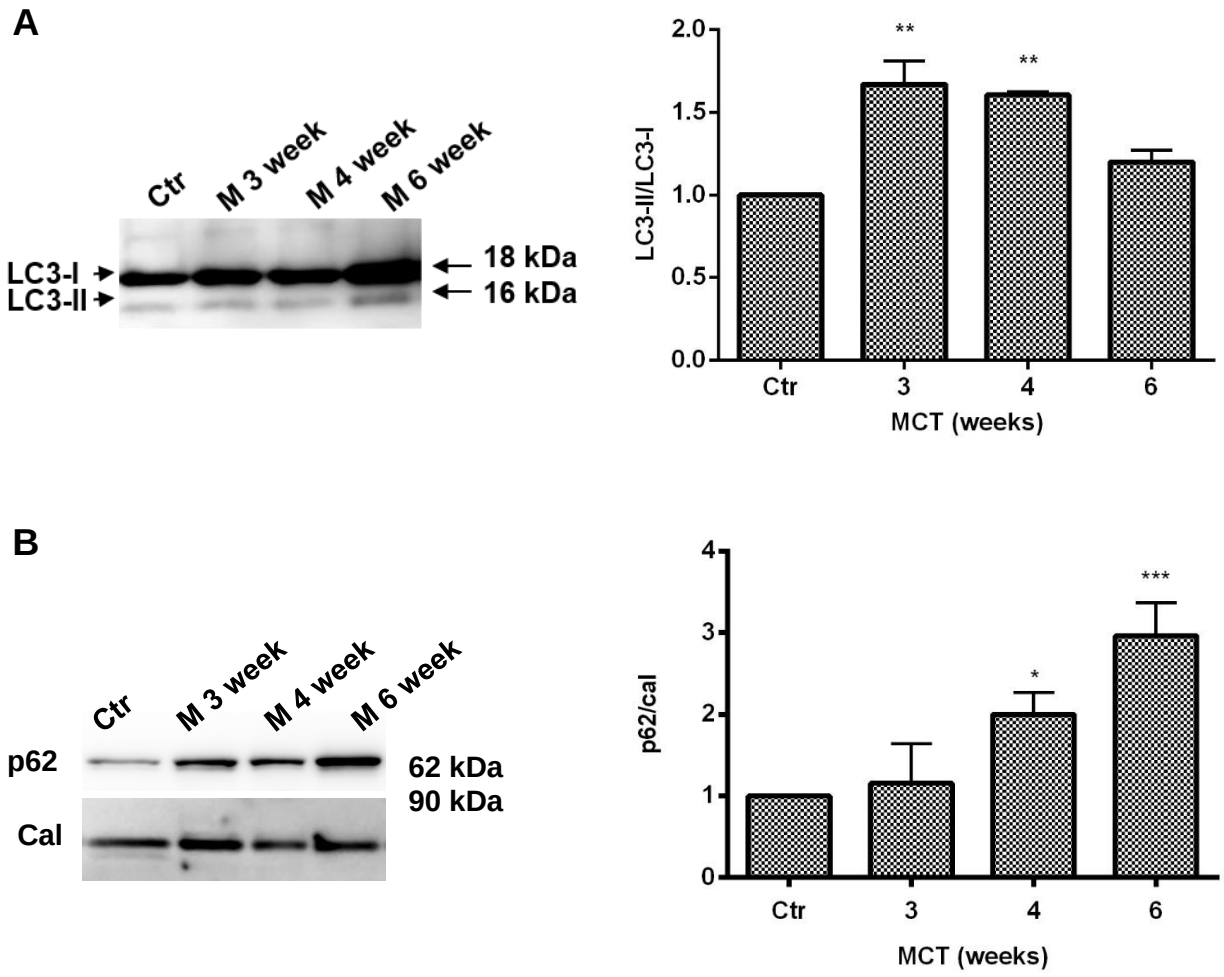

Figure 7. Effect on autophagy activity levels with progression of RV hypertrophy. RV homogenized from MCT-treated rat were prepared and analysed by western blotting using anti-LC3 antibody (A), anti-p62 antibody and anti-calnexin antibody as a loading control (B). The ratio LC3II/LC3I and p62 density was measured, plotted in a graph. Data are presented as the mean ± SEM of, at least 3 independent experiments and are expressed as a percentage of control. (*p < 0.05, **p < 0.01, ***p < 0.001 vs. Ctr.)

Cal, Calnexin; Ctr, Control;

Chapter 4. Discussion and Conclusion

PAH is characterised by a persistent elevation of pulmonary artery pressure that leads to an abnormal enlargement of the right ventricle, reflecting RVH. RVH is the main determinant of mortality in patients with PAH. Left untreated, PAH can result in heart failure and death. Although the understanding of PAH has expanded significantly in recent years, allowing the development of therapeutic approaches, a cure for this disease is far from being achieved. Therefore, further study is required to elucidate the molecular mechanisms underlying its pathophysiology, thus opening new avenues for the development of more efficient therapeutic strategies.

Although the exact pathophysiology underlying RVH remains unclear, inflammation may play an important role, contributing to contractility, vasoconstriction and proliferation of vascular cells, whilst also promoting vascular remodelling, the most significant feature of PAH (6, 20, 23). Furthermore, endothelial dysfunction in pulmonary vasculature results in an imbalance between the production and release of mediators, such as miRNA, that could modulate the integrity of right ventricular function. We have previously demonstrated (8) that hypoxia induces down-regulation of SMURF1 in cardiomyocytes through the secretion of miR-424(322) (8) by pulmonary artery endothelial cells (PAECs). Moreover, we also determined, in the MCT rat model of PH, the association between circulating miR-424(322) levels and the stage of right ventricle hypertrophy (8). In this study, we show that mediators secreted by ECs could modulate proteostasis and proteins levels in a cardiomyocyte.

LPS is a pathogen-associated molecular pattern, which can be found in the outer membrane of gram-negative bacteria (24, 25). Previous studies (26, 27) have reported that the mechanism of LPS-induced cardiac dysfunction is the activation of inflammation, necrosis or cardiomyocyte autophagy and, for this reason, has been extensively used to model inflammation-related diseases (27, 28). The rationale for this investigation was based on the recognition that PAH pathogenesis involves a variety of signalling pathways in transducing the inflammatory response. To examine whether LPS is able to stimulate inflammatory mediator production, through up-regulation of NF-κB, protein levels of the inflammatory marker IκBα were measured after LPS treatment on HUVECs. The results in this study show that IκBα decreased in cells treated with LPS. A decrease of IκBα proteins suggests that IκBα is being phosphorylated and degraded by the proteasome, evidencing that LPS could be used as a representation of the proinflammation condition in the disease state. Using HUVECs subjected to LPS as an *in vitro* model of ECs under inflammatory stress, Alamar Blue assay was performed to address if LPS concentrations

were affecting cell viability. It was found that the concentrations of LPS used had a non-cytotoxic effect on HUVECs.

Bearing in mind that the mechanism of LPS-induced cardiac dysfunction could be related with pro-inflammatory mediator release by ECs after LPS stimuli, it was beneficial to investigate how this stress condition modulates cardiomyocytes, the functional unit of the heart (29). Therefore, communication between ECs and cardiomyocytes is made through the secretion of paracrine signals and direct neighbouring cell contact (10). Cx43, a gap junction primarily found in ventricular cardiomyocytes, is necessary for the endothelial cell-to-cell communication (13). In order to assure the correct function of the heart, Cx43 needs to be carefully regulated by proteolytic systems (12). Identification of specific proteins that were modulated and how they are modulated during the development of PAH pathogenesis may contribute to a more effective approach for this disease. Failure to maintain the balance between accumulation and clearance can lead to abnormal protein aggregation and impaired protein degradation pathways (29). The two most important proteolytic systems in the heart are UPS, which usually degrades the majority of proteins, and autophagy, a biological lysosome-dependent process of degradation of long-lived or aggregated proteins and cellular organelles (30).

In the present work, the CM from HUVECs treated with LPS lead to a significant decrease in Cx43 protein levels in H9c2 cells. Using immunostaining, we were able to demonstrate that Cx43 is present closer to the nuclear region, compared with the control condition. These results suggest that mediators released by EC could induce internalisation of Cx43. When Cx43 is internalised into the cell, can be recycled back to the plasma membrane through recycling pathway, or it can be ubiquitinated for proteasomal and lysosomal degradation (31). To understand if modulation of Cx43 levels is via activation of the autophagy signalling pathway, LC3 and p62 were investigated in H9c2 cells. In H9c2 cells, the levels of p62 were significantly decreased and there is some evidence of an increase in LC3-II/LC3-I ratio, although without significance. Autophagy is a highly conserved cellular process where organelles and cytosolic proteins are encapsulated within double-membraned autophagosomes that ultimately fuse with lysosomes for degradation (32). A cytosolic form of LC3 (LC3-I) is conjugated to phosphatidylethanolamine to form LC3-phosphatidylethanolamine conjugate (LC3-II). This conversion of LC3-I into LC3-II, the recruitment of LC3-II to the autophagosome and the ratio of LC3-II/LC3-I constitute a reliable marker of autophagic activity (32). However, this ratio cannot differentiate increased autophagosome synthesis from decreased autophagosome degradation (19). For this reason, quantification of autophagy substrate

p62 is used as a reporter of autophagy activity (11), which inversely correlates with flux. In the literature, it has been reported that besides the role of LPS on inflammation, LPS stimulates cardiomyocyte autophagy, which may mediate cell death (26). Additionally, previous studies have demonstrated that Cx43 expression levels may be regulated by the autophagy pathway (12, 33), by recruitment of Cx43 to LC3-positive autophagosomes that subsequently fuse with the lysosome. Moreover, previous studies have shown that autophagic abnormalities are observed in PAECs, pulmonary artery smooth muscle cells (PASMCs) and in the right ventricular from both animal models and patients (2) and the autophagic marker LC3B and its activated form LC3B-II are increased in pulmonary tissues from patients with PH (2). In addition, Jing *et al* (20) demonstrated that inhibition of autophagy has protective effects on the pathological process of PAH, by suppressing the proliferation and migration of PASMCs and inducing their apoptosis. Together, this suggests that an inflammatory state could cause alteration of the expression levels and cellular distribution of Cx43 through autophagy. However, more studies are required to characterise the inflammatory signalling pathway between ECs, which release proinflammatory mediators, and cardiac cells.

Regarding disease, PAH is characterised by two stages of disease progression, an adaptative phase and a maladaptive phase, in which the signalling pathways are deregulated and cell homeostasis are seriously compromised. The RV initially compensates for the PH-induced increases in afterload through hypertrophy and increased contractile function. However, as PH continues to worsen, the RV's compensatory mechanisms fail, leading to RV failure and death. MCT administration and chronic exposure to hypoxia are the most widely used models of PAH in translational research, due to their good reproducibility and well-described histopathology (6). To elucidate the molecular mechanisms underlying this pathophysiology changes during the onset of PAH, we used the established MCT model. After 3-4 weeks of MCT administration in animals, the transition from an adaptive to a maladaptive phase occurs (21). Our results show an increase in expression level of Cx43 up to 4 weeks of disease progression, after which Cx43 levels decrease. Regarding the autophagy marker, the ratio of LC3-II/LC3-I seems to increase with disease development. However, converse to what was expected, the p62 levels, the data suggest an increase in the maladaptive stage, but without changes in the adaptative stage of disease. The results obtained in this study suggest that in our model of PAH there is a regulation of Cx43 levels, as well as the autophagy pathway. However, further study is necessary to understand how autophagy could be a suppressor or a promoter of the pathogenesis of PAH, which depends upon timing, magnitude, duration and severity of cellular stress (19).

Endothelial cells can be responsible for releasing soluble factors that can deliver cardio-injury signals to cardiomyocytes. In many different types of PH, deteriorating RV function is one of the strongest predictors of mortality. RV-directed therapies would strengthen the ability of the RV to adapt to the increased afterload, would inhibit maladaptive responses to improve the functional capacity, quality of life, and longevity of patients with PH. However, despite the critical importance of RV function to outcomes in PH, no RV-directed therapies exist. For this reason, more research to elucidate the two stages of disease progression are necessary.

Together, these results may clarify a mechanism of impairment on cardiac intercellular communication and consequently dysfunction of the heart, which could be used for the development of new therapeutic approaches in PH.

Chapter 5. References

1. Simonneau G, Montani D, Celermajer DS, Denton CP, Gatzoulis MA, Krowka M, et al. Haemodynamic definitions and updated clinical classification of pulmonary hypertension. Eur Respir J. 2019;53(1).
2. Chen YB. Autophagy and its role in pulmonary hypertension. Aging Clin Exp Res. 2019;31(8):1027-33.
3. Sun W, Chan SY. Pulmonary Arterial Stiffness: An Early and Pervasive Driver of Pulmonary Arterial Hypertension. Front Med. 2018;5:204.
4. Prins KW, Thenappan T. World Health Organization Group I Pulmonary Hypertension. Cardiology Clinics. 2016;34(3):363-74.
5. Galié N, Hoeper MM, Humbert M, Torbicki A, Vachiery J, Barbera J et al. Guidelines for the diagnosis and treatment of pulmonary hypertension: The Task Force for the Diagnosis and Treatment of Pulmonary Hypertension of the European Society of Cardiology (ESC) and the European Respiratory Society (ERS), endorsed by the International Society of Heart and Lung Transplantation (ISHLT). Eur Heart J 2009;30:2493-537.
6. Santos-Ribeiro D, Mendes-Ferreira P, Maia-Rocha C, Adao R, Leite-Moreira AF, Bras-Silva C. Pulmonary arterial hypertension: Basic knowledge for clinicians. Arch Cardiovasc Dis. 2016;109(10):550-61.
7. Humbert M, Guignabert C, Bonnet S, Dorfmuller P, Klinger JR, Nicolls MR, et al. Pathology and pathobiology of pulmonary hypertension: state of the art and research perspectives. Eur Respir J. 2019;53(1).
8. Baptista R, Marques C, Catarino S, Enguita FJ, Costa MC, Matafome P, et al. MicroRNA-424(322) as a new marker of disease progression in pulmonary arterial hypertension and its role in right ventricular hypertrophy by targeting SMURF1. Cardiovasc Res. 2018;114(1):53-64.
9. Lan NSH, Massam BD, Kulkarni SS, Lang CC. Pulmonary Arterial Hypertension: Pathophysiology and Treatment. Diseases. 2018;6(2).
10. Colliva A, Braga L, Giacca M, Zacchigna S. Endothelial cell-cardiomyocyte crosstalk in heart development and disease. J Physiol 00.0 2019;1–17.
11. Ribeiro-Rodrigues TM, Martins-Marques T, Morel S, Kwak BR, Girao H. Role of connexin 43 in different forms of intercellular communication - gap junctions, extracellular vesicles and tunnelling nanotubes. J Cell Sci. 2017;130(21):3619-30.
12. Wang GY, Bi YG, Liu XD, Han JF, Wei M, Zhang QY. Upregulation of connexin 43 and apoptosis associated protein expression by high glucose in H9c2 cells was improved by resveratrol via the autophagy signalling pathway. Mol Med Rep. 2017;16(3):3262-8.

13. Kells-Andrews RM, Margraf RA, Fisher CG, Falk MM (2018) Connexin-43 K63-polyubiquitylation on lysines 264 and 303 regulates gap junction internalization. J Cell Sci. 2018;131.
14. Dempsie Y, Martin P, Upton PD. Connexin-mediated regulation of the pulmonary vasculature. Biochem Soc Trans. 2015;43(3):524-9.
15. Kocaturk NM, Gozuacik D. Crosstalk Between Mammalian Autophagy and the Ubiquitin-Proteasome System. Front Cell Dev Biol. 2018;6:128.
16. Lilienbaum A. Relationship between the proteasomal system and autophagy. Int J Biochem Mol Biol 2013;4(1):1-26.
17. Liu T, Zhang L, Joo D, Sun SC. NF-κB signalling in inflammation. Signal Transduct Target Ther. 2017;2(e17023):1-9.
18. Chen L, Deng H, Cui H, Fang J, Zuo Z, Deng J, et al. Inflammatory responses and inflammation-associated diseases in organs. Oncotarget, 2018;9(6):7204-7218.
19. Chen R, Jiang M, Li B, Zhong W, Wang Z, Yuan W, et al. The role of autophagy in pulmonary hypertension: a double-edge sword. Apoptosis. 2018;23(9-10):459-69.
20. Jing X, Jiang T, Dai L, Wang X, Jia L, Wang H, et al. Hypoxia-induced autophagy activation through NF-κB pathway regulates cell proliferation and migration to induce pulmonary vascular remodeling. Exp Cell Res. 2018;368(2):174-83.
21. Frump AL, Bonnet S, de Jesus Perez VA, Lahm T. Emerging role of angiogenesis in adaptive and maladaptive right ventricular remodeling in pulmonary hypertension. Am J Physiol Lung Cell Mol Physiol. 2018;314(3):L443-L60.
22. Gomez-Arroyo JG, Farkas L, Alhussaini AA, Farkas D, Kraskauskas D, Voelkel NF, et al. The monocrotaline model of pulmonary hypertension in perspective. Am J Physiol Lung Cell Mol Physiol 2012;302:L363–L369.
23. Huertas A, Guignabert C, Barbera JA, Bartsch P, Bhattacharya J, Bhattacharya S, et al. Pulmonary vascular endothelium: the orchestra conductor in respiratory diseases: Highlights from basic research to therapy. Eur Respir J. 2018;51(4).
24. Maldonado RF, Sa-Correia I, Valvano MA. Lipopolysaccharide modification in Gram-negative bacteria during chronic infection. FEMS Microbiol Rev. 2016;40(4):480-93.
25. Park BS, Lee JO. Recognition of lipopolysaccharide pattern by TLR4 complexes. Exp Mol Med. 2013;45(e66):1-9.
26. Li X, Liu J, Wang J, Zhang D. Luteolin suppresses lipopolysaccharide induced cardiomyocyte hypertrophy and autophagy in vitro. Mol Med Rep. 2019;19(3):1551-60.
27. Ranneh Y, Akim AM, Hamid HA, Khazaai H, Mokhtarrudin N, Fadel A, et al. Induction of Chronic Subclinical Systemic Inflammation in Sprague-Dawley Rats

Stimulated by Intermittent Bolus Injection of Lipopolysaccharide. Arch Immunol Ther Exp. 2019;67(6):385-400.

28. Noailles A, Maneu V, Campello L, Lax P, Cuenca N. Systemic inflammation induced by lipopolysaccharide aggravates inherited retinal dystrophy. Cell Death Dis. 2018;9(3):350.

29. Wu B, Yu L, Wang Y, Wang H, Li C, Yin Y et al. Aldehyde dehydrogenase 2 activation in aged heart improves the autophagy by reducing the carbonyl modification on SIRT1. Oncotarget, 2016;7(3):2175-2188.

30. Chen RH, Chen YH, Huang TY. Ubiquitin-mediated regulation of autophagy. J Biomed Sci. 2019;26(1):80.

31. Ribeiro-Rodrigues TM, Catarino S, Pinho MJ, Pereira P, Girao H. Connexin 43 ubiquitination determines the fate of gap junctions: restrict to survive. Biochem Soc Trans. 2015;43(3):471-5.

32. Zhang CF, Zhao FY, Xu SL, Liu J, Xing XQ, Yang J. Autophagy in pulmonary hypertension: Emerging roles and therapeutic implications. J Cell Physiol. 2019;234(10):16755-67.

33. Martins-Marques T, Catarino S, Zuzarte M, Marques C, Matafome P, Pereira P, et al. Ischaemia-induced autophagy leads to degradation of gap junction protein connexin43 in cardiomyocytes. Biochem J. 2015;467(2):231-45.